Hindawi
International Journal of Aerospace Engineering
Volume 2021, Article ID 9912618, 13 pages
https://doi.org/10.1155/2021/9912618

Research Article

The Investigation on L_1 Adaptive Control of the Tilt-Rotor Aircraft

Quanlong Chen,[1] Shanyong Zhao,[2] Ke Lu,[2,3] Senkui Lu,[2] Chunsheng Liu,[4] and Renliang Chen[3]

[1]*College of Aerospace Engineering, Chongqing University, Chongqing 400044, China*
[2]*Science and Technology on Rotorcraft Aeromechanics Laboratory, China Helicopter Research and Development Institute, Jingdezhen, Jiangxi 333001, China*
[3]*National Key Laboratory of Science and Technology on Rotorcraft Aeromechanics, Nanjing University of Aeronautics and Astronautics, Nanjing, Jiangsu 210016, China*
[4]*College of Automation Engineering, Nanjing University of Aeronautics and Astronautics, Nanjing, Jiangsu 210016, China*

Correspondence should be addressed to Ke Lu; looknuaa@nuaa.edu.cn

Received 20 March 2021; Revised 5 May 2021; Accepted 29 May 2021; Published 21 June 2021

Academic Editor: Youmin Zhang

Considering the uncertainty of the flight dynamics model of the tilt-rotor aircraft in different flight modes, an L_1 adaptive controller for full flight modes control system of tilt-rotor aircraft is designed. Taking advantage of the separation of robustness and adaptive design of the L_1 adaptive controller, adaptive gain, and low-pass filter are designed to achieve the desired control performance and meet the requirements of flight quality. The simulations of XV-15 tilt-rotor aircraft in helicopter mode and airplane mode are carried out. Then, the simulation of conversion mode is further carried out. The results show that the tilt-rotor aircraft can track the reference signal well under the L_1 control system. In addition, the changes of states as well as controls in conversion mode flight are quite smooth which is very meaningful for engineering application.

1. Introduction

A tilt-rotor aircraft has the advantages of both fixed-wing and rotorcraft such as high speed and long-range flight, vertical take-off, and landing ability. It can cover the flight envelope of conventional helicopters and propeller planes and has broad applications in both civil and military fields. However, due to the integration of flight modes and control modes of fixed-wing aircraft and helicopters, tilt-rotor aircraft has helicopter mode, conversion mode, and airplane mode, as shown in Figure 1. It is a typical morphing aircraft. Therefore, the mathematical model of flight dynamics is highly nonlinear. It is much more complicated in flight control system design compared with other aircraft.

Since the promulgation of ADS-33E-PRF, preliminary studies on flight control of tilt-rotor aircraft mainly focus on stability enhancement system design and quality improvement [1–4]. Juhasz developed a high order rotorcraft mathematical mode against a large civil tilt-rotor concept. At the same time, the corresponding control system is designed to meet the quality requirements [5]. In Ref. [6], neural network controller was used to accomplish the neural network path-tracking and real-time multitask flight simulation for the automatic transition of tilt-rotor aircraft. The flight performance of conversion mode is evaluated based on the linearized model. Rysdyk and Calise [7] propose an inverse control method based on neural network model to control civil tilt-rotor aircraft, which can ensure satisfied dynamic performance in the whole flight envelope. The stability of the system and the boundary of tracking error are strictly proved based on Lyapunov theory. Choi et al. [8] divide the nacelle angle into 90-60 degrees for helicopter mode, 60-30 degrees for conversion mode, and 30-0 degrees for airplane mode in the flight control system of unmanned tilt-rotor aircraft. The way of control scheduling is used, which is easy to be implemented in engineering. Lee et al. [9] divide the tilt-rotor aircraft into different operating points based on discretization and optimize the control law parameters at different operating points using particle swarm optimization algorithm. In Ref. [10], based on an optimal control concept, an

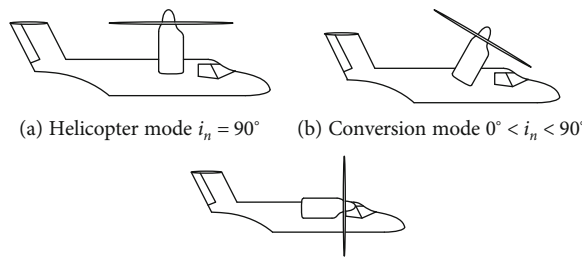

(a) Helicopter mode $i_n = 90^\circ$ (b) Conversion mode $0^\circ < i_n < 90^\circ$

(c) Airplane mode $i_n = 0^\circ$

Figure 1: Tilt-rotor aircraft three flight modes.

online optimization control method was developed for the tilt-rotor UAV. In Ref. [11], a smooth switching control scheme is provided for the tilt-rotor aircraft. However, the flight mechanic model in the above literature has been simplified to a large extent. As a result, the simulation results cannot reflect the real performance of the controllers. For a class of singularly perturbed Markov jump descriptor systems with nonlinear perturbation, a stochastic integral sliding mode control strategy is developed in [12, 13]. In aeronautical engineering application field, the L_1 adaptive control has attracted wide attention in recent years. It is modified on the basis of the classical model reference adaptive control [14–17]. A low pass filter is introduced to decouple the adaptive and robustness of the control system, a larger adaptive gain can be adopted to improve the parameter estimation speed and obtain better control performance. The corresponding test work has been carried out, especially in the field of aerospace [18–23].

Motivated by the discussions above, we introduce the L_1 adaptive control method to the tilt-rotor aircraft in the flight control system. The major limitations for its applications can be summarized as follows:

(1) The dynamics of tilt-rotor aircraft are usually highly nonlinear and coupled, and it has multiple flight modes. It is still a challenging problem to get desired dynamic performance for the controlled system in the full envelope

(2) The performance of tilt-rotor aircraft control system should meet the related requirements in flight quality specification

(3) The design of controller parameters should fully consider the physical realizability of the aircraft

The paper is organized as follows. Section 2 introduces the mathematical model. Section 3 gives the L_1 adaptive controller design. Section 4 presents simulation studies. Finally, Section 5 draws the conclusion.

2. Mathematical Model Description and Verification

2.1. Model Description. The flight dynamics model is the basis for the analysis of flight characteristics of the aircraft and flight control system design. XV-15 tilt-rotor aircraft is chosen forth research object, and its basic parameters are shown in Table 1. The flight dynamics model of tilt-rotor aircraft is established.

Table 1: Basic parameters of XV-15 tilt-rotor.

Parameters value	
Weight (m)	5897 kg
Rotor radius (R)	3.81 m
Blade number (N_b)	3×2
Blade twist (θ_t)	-41°
Rotor speed (Ω)	589 rpm (helicopter mode) 517 rpm (airplane mode)
Lock number (γ)	3.83
Solidity (σ)	0.089
Pitch-flap coupling angle (δ_3)	15°
Flapping hinge restraint K_β	17476 Nm/rad
Flap moment of inertia (I_β)	139 kg·m^2
Nacelle length (d)	1.4 m
Wing area (S_w)	16.82 m^2
Horizontal tail areas (S_{ht})	4.67 m^2
Vertical tail areas (S_{vt})	2.35 m^2

In the modeling of flight mechanics, tilt-rotor aircraft adopts component aerodynamic modeling method, and the rotor aerodynamic modeling is the focus of the entire modeling work.

The main aeromechanic features in the XV-15 model are listed below:

(1) Rigid prop-rotor blades with nonlinear, quasisteady aerodynamics in table look-up form as functions of the angle of attack and Mach number

(2) Finite-state rotor inflow model with 13 inflow states in total for each rotor

(3) The wing/flap lift, drag, and pitching moment coefficients are defined as functions of the angle of attack, nacelle angle, and flap setting obtained by matching experimental data

(4) Rotor-wing-empennage interaction modeled was determined from wind tunnel experiment

(5) Nonlinear fuselage aerodynamics is functions of the angle of attack and sideslip

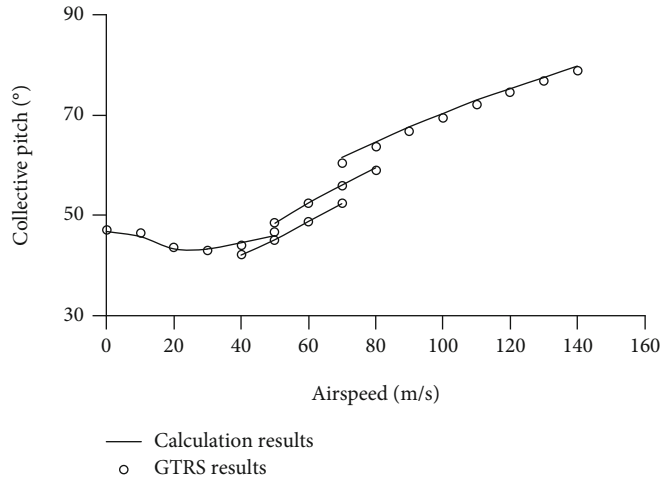

Figure 2: Collective pitch trim validation.

(6) Empennage aerodynamics is modeled in a similar manner to the main wing

The XV-15 tilt-rotor aircraft uses both helicopter and airplane control strategies to control the aircraft. In helicopter flight mode, longitudinal cyclic, differential collective, and differential longitudinal cyclic are used to pitch, roll, yaw, and heave control, respectively. As the tilt-rotor aircraft converts from helicopter flight mode to airplane flight mode, the helicopter rotor control surfaces are washed out as a function of nacelle angle and flight speed.

The tilt-rotor aircraft flight dynamics model could be given by

$$\dot{\mathbf{X}} = \mathbf{f}(\mathbf{X}, t) + \mathbf{g}(\mathbf{X}, t)\mathbf{u}. \tag{1}$$

The state variables are given in the form of a vector $\mathbf{X} \in R^{47\times1}$, which includes 26 rotor inflow states, 12 flapping motion states, and 9 aircraft states. $\mathbf{u} \in R^{4\times1}$ denotes a vector constituting the control inputs. The model detail can refer to Ref [24] (Ke Lu and C. S. Liu).

2.2. Mode Validation

2.2.1. Trim Result Validation. In the trim validation, the control inputs at different nacelle incidence angles are compared with simulation results from GTRS reports [25]. Figures 2 and 3, respectively, show the comparison of collective pitch and longitudinal control.

According to Figures 2 and 3, in helicopter mode, the variation trend of collective pitch is similar to the conventional helicopter. The collective pitch has the characteristic bucket profile as a function of flight speed. In airplane mode, the function of the rotor is providing forward pull force to overcome fuselage drag. That is to say, the wing is able to generate enough lift to overcome gravity. The collective pitch is much larger than that of the helicopter mode. In addition, longitudinal control input increases with speed in all flight modes. Overall, the calculation results are quite consistent with GTRS results in all flight modes under the trim condition.

2.2.2. Linearized Result Validation. With the application of a linearization algorithm, the rotor and inflow modes residualized out via quasistatic reduction, and then the nonlinear equation can be reduced to the form of

$$\dot{\mathbf{x}} = \mathbf{A}\mathbf{x} + \mathbf{B}\mathbf{u}, \tag{2}$$

$$\mathbf{x} = [u, v, w, p, q, r, \phi, \theta, \psi], \tag{3}$$

$$\mathbf{u} = \left[\delta_{\text{coll}}, \delta_{\text{long}}, \delta_{\text{lat}}, \delta_{\text{ped}}\right]. \tag{4}$$

To linearization validation, a comparison of the eigenvalues for matrix A in equation (2) with results from the flight test and GTRS is shown in Tables 2 and 3. As shown in Table 2, the characteristic in helicopter mode of the eigenvalue distribution between calculation results in this paper and flight test are very similar. In particular, for phugoid and dutch roll modes, calculation results in this paper and flight test have given the conclusion of instability. The airplane mode eigenvalues are shown in Table 3. In general, the calculation results in this paper are closer to GTRS, especially the prediction of short period modes.

2.2.3. Control Response Validation. The control response verification is mainly to verify whether the response of tilt-rotor aircraft conforms to the laws of physics under the excitation of the control input. In this section, GTRS data is used to verify the control response of the tilt-rotor aircraft.

In the helicopter mode, the longitudinal stick in the hovering state is pushed forward by 5%, and the time response of the pitch angle and rate is shown in Figures 4 and 5. It can be seen from the figure that when the longitudinal stick is pushed forward and causes the aircraft head down, which conforms to the basic physical characteristics of the aircraft. In addition, the calculation model in this paper has the same trend and similar amplitude with the GTRS data.

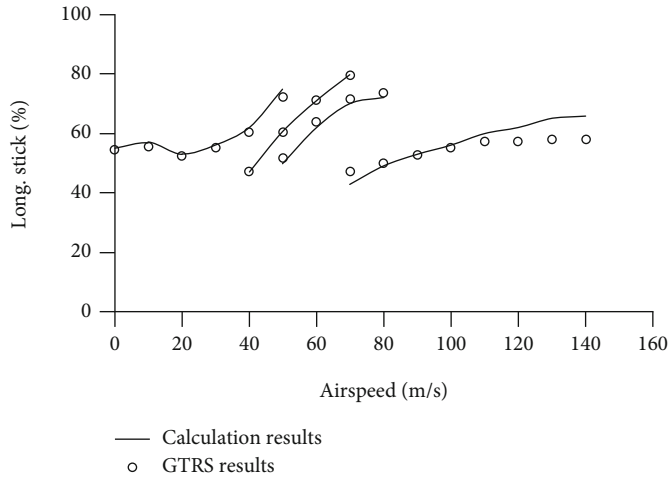

Figure 3: Longitudinal stick trim validation.

Table 2: Hover mode eigenvalues validation.

Hover mode	Natural mode	Calculated	Flight data
Longitudinal	Phugoid	$0.2981 \pm 0.7555i$	$0.2681 \pm 0.5132i$
	Pitch subsidence	-1.0	-1.32
	Heave subsidence	-0.17	-0.105
Lateral	Dutch roll	$0.1866 \pm 1.0826i$	$0.1868 \pm 0.4061i$
	Spiral subsidence	-0.1609	-0.102
	Roll subsidence	-2.6539	-1.23

Table 3: Airplane mode ($V = 200$ kt) eigenvalues validation.

Hover mode	Natural mode	Calculated	GTRS
Longitudinal	Phugoid	$-0.2111 \pm 0.2625i$	$-0.2115 \pm 0.1576i$
	Short-period pitch	$-1.7402 \pm 3.9172\,i$	$-1.6948 \pm 3.4555i$
Lateral	Dutch roll	$-0.6525 \pm 2.2092i$	$-0.4989 \pm 3.4555i$
	Spiral subsidence	-0.1384	-0.1226
	Roll subsidence	-0.7128	-1.0649

In conclusion, the calculated values in this paper are in good agreement with those in the GTRS. In brief, the XV-15 tilt-rotor flight dynamics model is proved to be valid. So we have enough confidence in the following controller design.

3. L_1 Adaptive Controller Design

3.1. Problem Description. The mathematical model of the pitch channel of the tilt-rotor aircraft can be described by the following formula

$$\begin{aligned} \dot{x}(t) &= A_m x(t) + b(\omega u(t) + f(t, x(t), \xi(t))), x(0) = x_0, \\ \dot{x}_\xi(t) &= g\left(t, x_\xi(t), x(t)\right), x_\xi(0) = x_{\xi 0}, \\ \xi(t) &= h\left(t, x_\xi(t)\right), \\ y(t) &= c^\top x(t), \end{aligned} \tag{5}$$

where $x(t) = [\theta, q]^T$ is the pitch angle and pitch angle velocity, respectively; $A_m \in \mathbb{R}^{2\times 2}$ is a known Hurwitz matrix whose characteristics meet the specifications of flight quality; $b, c \in \mathbb{R}^2$ is known constant vectors; $u(t) \in \mathbb{R}$ is control input; ω is control efficiency; $f(t, x(t), \xi(t))$ is unknown nonlinear dynamic mapping; $x_\xi(t)$ and $\xi(t)$ are the state and output of unmodeled dynamics, respectively, and $g(\cdot)$ and $h(\cdot)$ are nonlinear mappings of corresponding dimensions.

3.2. L_1 Adaptive Control System Design. The system above is subject to the following assumptions:

Assumption 1. (Boundedness of $f_i(t, 0)$) There exists Bi > 0, such that $\|f_i(t, 0)\|_\infty \le B_i$ holds for $t \ge 0$ and for $i = 1, 2$.

Assumption 2. (Semiglobal Lipschitz condition) For arbitrary$\delta > 0$, there exist positive $K_{1\delta}, K_{2\delta}$, such that

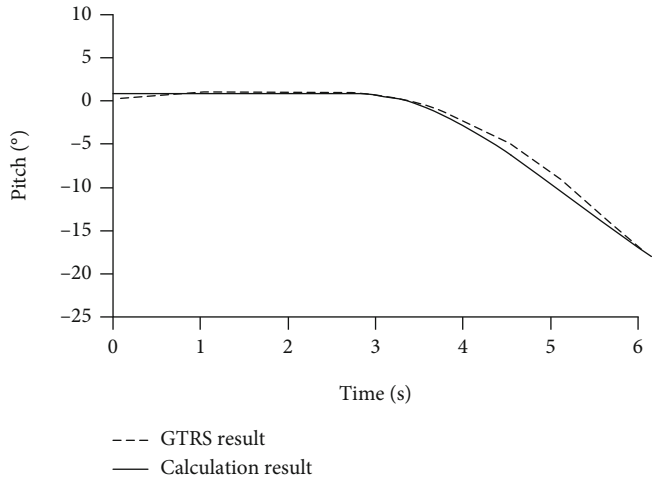

Figure 4: Pitch angle step response in helicopter mode (hover).

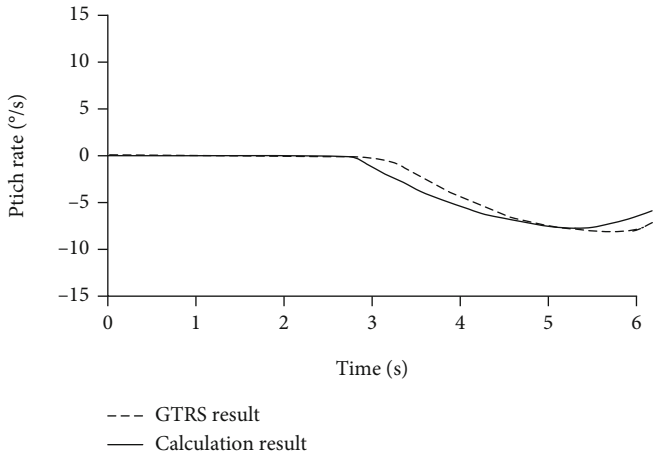

Figure 5: Pitch rate step response in helicopter mode (hover).

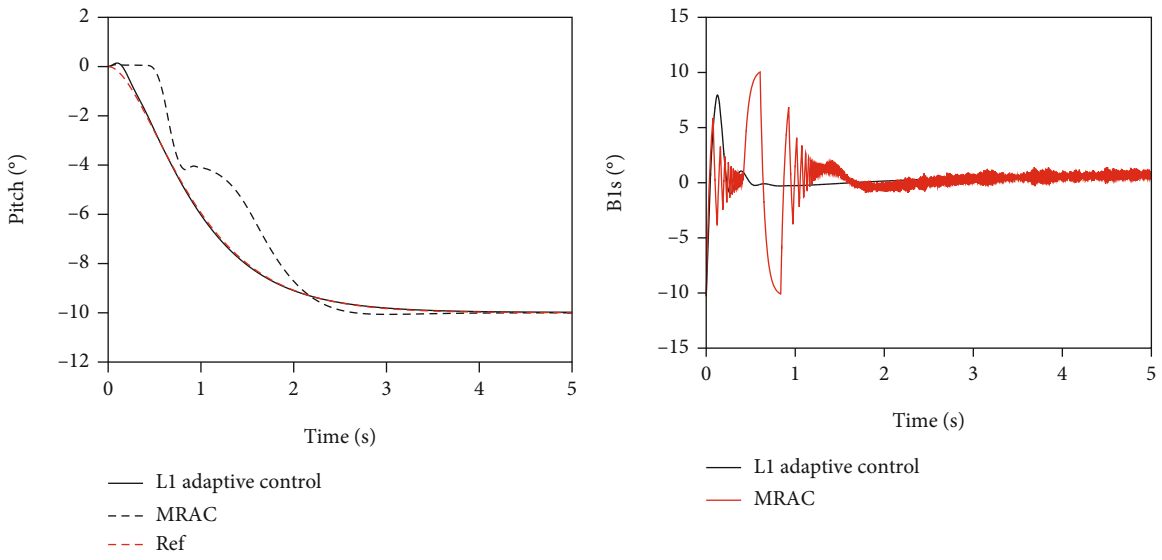

(a) Pitch angle change curve

(b) Longitudinal cycle pitch change curve

Figure 6: The pitch angle and longitudinal cycle for helicopter mode.

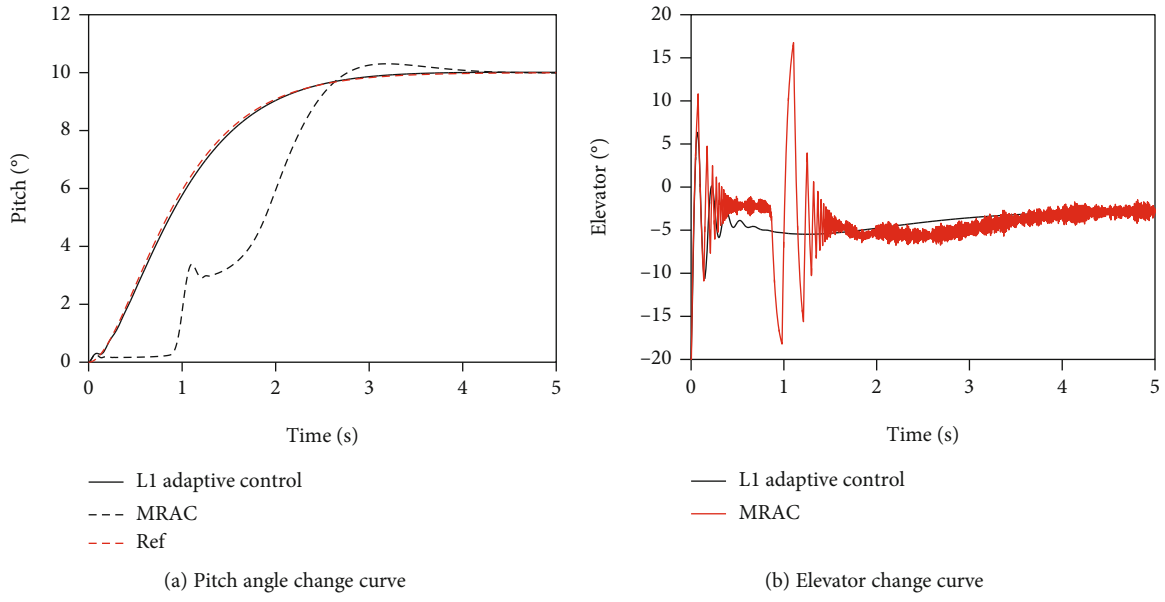

(a) Pitch angle change curve (b) Elevator change curve

Figure 7: The pitch angle and elevator for airplane mode.

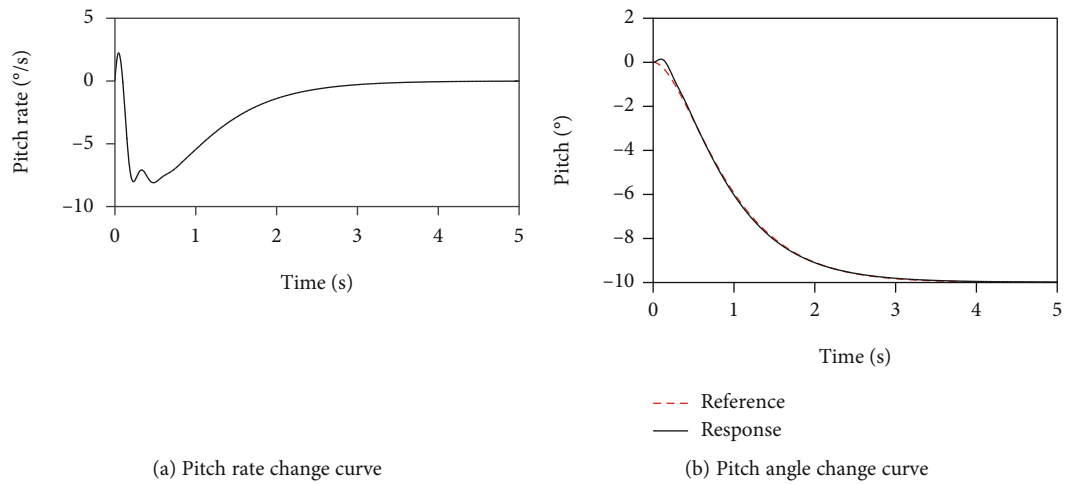

(a) Pitch rate change curve (b) Pitch angle change curve

Figure 8: The pitch rate and pitch angle of step response.

$\|f_i(t,x_1) - f_i(t,x_2)\|_{\infty} \le K_{i\delta}\|x_1 - x_2\|_{\infty}$, $i = 1, 2$, for all $\|x_j\|_{\infty} \le \delta, j = 1, 2$, uniformly in t.

Assumption 3. (Stability of unmodeled dynamics) The x_ξ -dynamics are BIBO stable with respect to both initial conditions $x_{\xi 0}$ and input$x(t)$.

In this study, the uncertainties are mainly caused by aerodynamic parameters. They are always uniformly bounded and limited in how fast they can change. Thus, these assumptions are reasonable.

The state prediction system, adaptive law, and control law of the L_1 adaptive control system of the tilt-rotor aircraft are designed as follows.

3.2.1. State Prediction System.

$$\begin{aligned}\dot{\hat{x}}(t) &= A_m\hat{x}(t) + b\left(\hat{\omega}(t)u(t) + \hat{\lambda}(t)\|x_t\|_{\mathcal{L}_\infty} + \hat{\sigma}(t)\right),\\ \hat{x}(0) &= x_0,\\ \hat{y}(t) &= c^{\top}\hat{x}(t),\end{aligned} \tag{6}$$

where $\hat{x}(t) \in \mathbb{R}^n$ is the state estimate of the system, and $\hat{\omega}(t) \in \mathbb{R}$, $\hat{\lambda}(t) \in \mathbb{R}$, $\hat{\sigma}(t) \in \mathbb{R}$ is the adaptive parameter estimates.

3.2.2. Adaptive Law.

$$\begin{aligned}\dot{\widehat{\omega}}(t) &= \Gamma \mathrm{Proj}\left(\widehat{\omega}(t), -\tilde{x}^{\top}(t)Pbu(t)\right), \widehat{\omega}(0) = \widehat{\omega}_0,\\ \dot{\widehat{\lambda}}(t) &= \Gamma \mathrm{Proj}\left(\widehat{\lambda}(t), -\tilde{x}^{\top}(t)Pb\|x_t\|_{\mathscr{L}_\infty}\right), \widehat{\lambda}(0) = \widehat{\lambda}_0,\\ \dot{\widehat{\sigma}}(t) &= \Gamma \mathrm{Proj}\left(\widehat{\sigma}(t), -\tilde{x}^{\top}(t)Pb\right), \widehat{\sigma}(0) = \widehat{\sigma}_0,\end{aligned} \tag{7}$$

where $\tilde{x}(t) \triangleq \widehat{x}(t) - x(t)$; $\Gamma \in \mathbb{R}^+$ is the adaptive gain; $P = P^{\top} > 0$ is the solution of the Lyapunov equation $A_m^{\top}P + PA_m = -Q$, and $Q = Q^{\top} > 0$; Proj is the projection operator.

3.2.3. Control Law.

$$u(s) = -kD(s)\left(\widehat{\eta}(s) - k_g r(s)\right), \tag{8}$$

where $r(s)$ is the Laplace transform of $r(t)$, $k_g \triangleq -1/(c^{\top}A_m^{-1}b)$, k is the design parameter of the low-pass filter, $D(s)$ generally takes the form of integral, where $\widehat{\eta}(s)$ is the Laplace transform of the following formula

$$\widehat{\eta}(t) \triangleq \widehat{\omega}(t)u(t) + \widehat{\lambda}(t)\|x(t)\|_{\infty} + \widehat{\sigma}(t). \tag{9}$$

The adaptive control signal passes through the low-pass filter shown in the following equation before entering the actual system.

$$C(s) \triangleq \frac{\omega k D(s)}{1 + \omega k D(s)}, \tag{10}$$

where $C(s)$ is a filter that satisfies $C(0) = 1$ and satisfies the following L_1 adaptive stability conditions.

Theorem 4. *For system (5), given a ρ_0, there is $\rho_r > \rho_{in}$. When the system adopts the abovementioned state prediction system, adaptive law, and control law, the system is closed-loop stable when the following norm inequality is satisfied.*

$$\|G(s)\|_{\mathscr{L}_1} < \frac{\rho_r - \left\|H(s)C(s)k_g\right\|_{\mathscr{L}_1}(r)_{\mathscr{L}_\infty} - \rho_{in}}{L_{\rho_r}\rho_r + B}, \tag{11}$$

where $G(s) \triangleq H(s)(1 - C(s))$, $H(s) \triangleq (s\mathbb{I} - A_m)^{-1}b$, $\rho_{in} \triangleq \|s(s\mathbb{I} - A_m)^{-1}\|_{\mathscr{L}_1}\rho_0$, $L_{\rho_r} \triangleq \bar{\rho}_r(\rho_r)/\rho_r d_{f_x}(\bar{\rho}_r(\rho_r))$, *and* $\bar{\rho}_r(\rho_r) \triangleq \max[\rho_r + \bar{\gamma}_1, L_1(\rho_r + \bar{\gamma}_1) + L_2]$.

3.3. L_1 Adaptive Control System Analysis. In order to analyze the closed-loop characteristics of the system, the following closed-loop reference system is defined

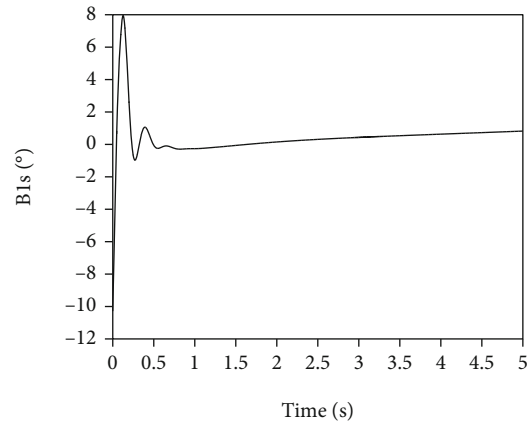

Figure 9: Longitudinal cycle pitch change curve.

$$\begin{aligned}\dot{x}_{\mathrm{ref}}(t) &= A_m x_{\mathrm{ref}}(t) + b(\omega u_{\mathrm{ref}}(t) + f(t, x_{\mathrm{ref}}(t), \xi(t))),\\ x_{\mathrm{ref}}(0) &= x_0,\\ u_{\mathrm{ref}}(s) &= \frac{C(s)}{\omega}\left(k_g r(s) - \eta_{\mathrm{ref}}(s)\right),\\ y_{\mathrm{ref}}(t) &= c^{\top}x_{\mathrm{ref}}(t),\end{aligned} \tag{12}$$

where $\eta_{\mathrm{ref}}(t) \triangleq f(t, x_{\mathrm{ref}}(t), \xi(t))$.

Lemma 5. *When the closed-loop reference system satisfies the stability condition, for any $\tau > 0$*

$$\|\xi_\tau\|_{\mathscr{L}_\infty} \le L_1\left(\left\|x_{ref\,\tau}\right\|_{\mathscr{L}_\infty} + \gamma_1\right) + L_2, \tag{13}$$

$$\left\|x_{ref}\right\|_{\mathscr{L}_\infty} \le \rho_r, \left\|u_{ref}\right\|_{\mathscr{L}_\infty} \le \rho_{ur}. \tag{14}$$

That is, the closed-loop reference system is BIBS stable.

Lemma 6. *For system (5), when the system adopts the state prediction system, adaptive law, and control law and satisfies the stability condition (14), if the adaptive gain Γ is chosen to verify the lower bound*

$$\Gamma \ge \frac{\rho_m(\rho, \rho_u, \rho_{\dot{u}})}{\lambda_{\min}(P)\gamma_0^2}. \tag{15}$$

Then, the following inequality holds

$$\|\tilde{x}\|_{\mathscr{L}_\infty} < \gamma_0. \tag{16}$$

Then, we have

$$\left\|x_{ref} - x\right\|_{\mathscr{L}_\infty} < \gamma_1, \tag{17}$$

$$\left\|u_{ref} - u\right\|_{\mathscr{L}_\infty} \le \gamma_2, \tag{18}$$

where γ_1 and γ_2 are dependent on $f_i(t, x)$ bounds and L_1 controller design parameters.

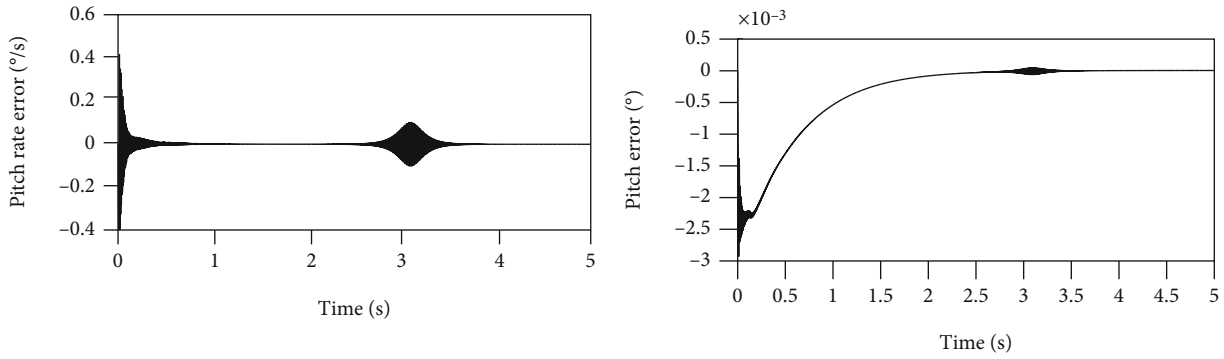

(a) Pitch rate prediction error (b) Pitch angle prediction error

Figure 10: The state prediction error change curves of step response.

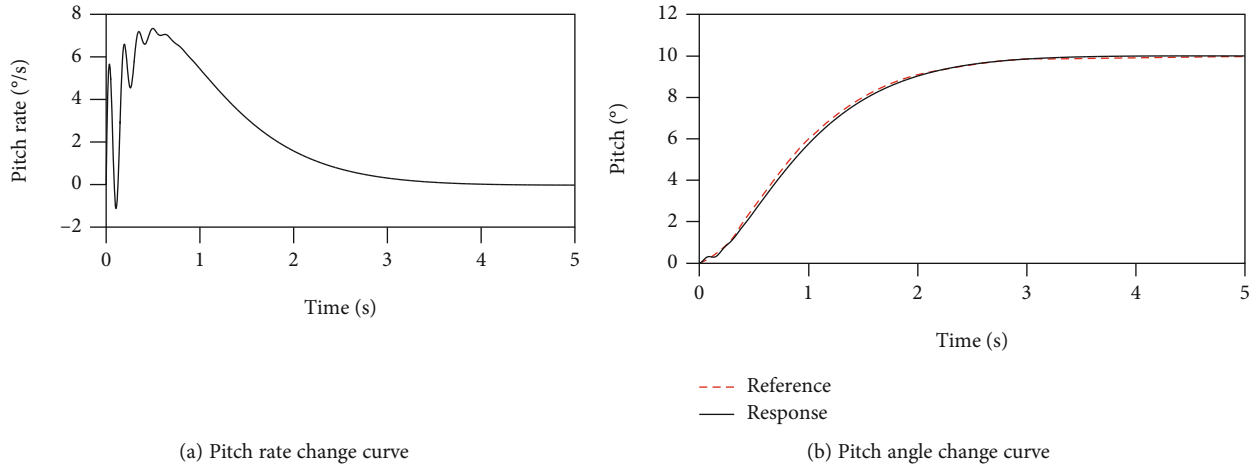

(a) Pitch rate change curve (b) Pitch angle change curve

Figure 11: The pitch rate and pitch angle of step response.

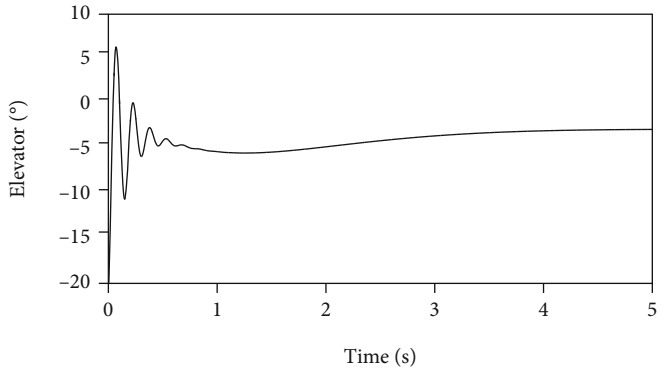

Figure 12: Elevator change curve.

Remark 1. As the adaptive gain Γ goes to infinity, the system (5) will follow the reference system (12) arbitrarily closely. It implies that the performance limitations are consistent with the hardware limitations.

3.4. Command System Design. ADS-33E-PRF flight quality specification specifies a variety of response types. These response types are the guarantee for the helicopter to complete high-quality flight missions. The most basic is the angular rate response type and the attitude response type. In general, the aircraft basically has the angular rate response type through the preliminary stabilization system. In order to reduce the pilot workload, Attitude Command/Attitude Hold response type control system is designed for the longitudinal pitch channel.

According to ADS-33E-PRF flight quality specification, the flight quality constraint parameters of the attitude command type are the bandwidth and phase delay index for small-scale high-frequency attitude changes and the quickness index for medium attitude changes.

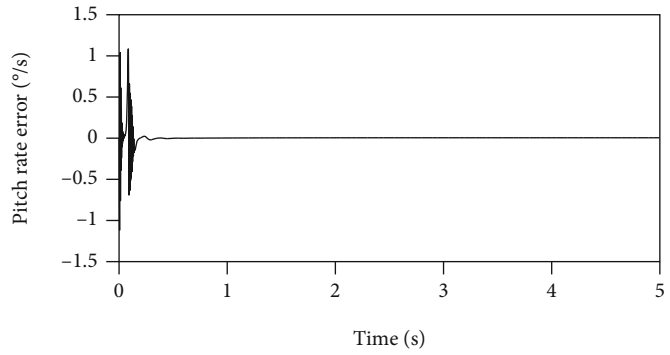

(a) Pitch rate prediction error

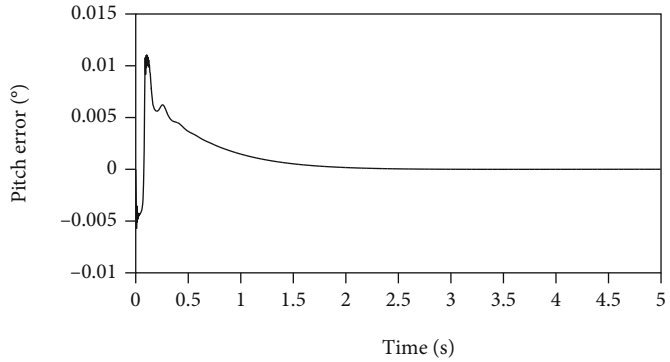

(b) Pitch angle prediction error

Figure 13: The state prediction error change curve of step response.

The following transfer function is used to design the pitch attitude command model.

$$\frac{\theta_{\text{com}}(s)}{\delta_{\text{long}}(s)} = \frac{K_{\text{AC}}}{(1/\omega^2)s^2 + (2\zeta/\omega)s + 1} e^{-\tau_{\text{SL}}s}. \tag{19}$$

According to the definition of bandwidth and phase delay in the ADS-33E-PRF flight quality specification, the relationship between the phase bandwidth ω_{BW} of the attitude command model and the command model parameters ω, ζ, and τ_{SL} are as follows.

$$\tan\left(\frac{\pi}{4} + \tau_{\text{SL}}\omega_{\text{BW}}\right) - \frac{2\zeta\omega_{\text{BW}}\omega}{\omega_{\text{BW}}^2 - \omega^2} = 0. \tag{20}$$

Phase delay τ_{P}

$$\tau_{\text{p}} = \frac{2\omega_{180}\tau_{\text{SL}} - \arctan\left(4\zeta\omega_{180}\omega/4\omega_{180}^2 - \omega^2\right)}{2\omega_{180}}, \tag{21}$$

where ω_{180} is the frequency corresponding to equation (19) when the phase of the transfer function is 180 deg, which can be obtained by solving the following equation.

$$\tan\left(\tau_{\text{SL}}\omega_{180}\right) - \frac{2\zeta\omega_{180}\omega}{\omega_{180}^2 - \omega^2} = 0. \tag{22}$$

According to the corresponding relationship between response types and mission task recommended in the ADS-33E-PRF flight quality specification, the attitude response type is generally the response type used in complex situations such as degraded visual environment. At the same time, in the case of divided attention operation, the specification has made stricter requirements on the damping ratio of the medium period response. Therefore, the damping ratio of 1 is chosen. In this case, the quickness index of equation (19) is as follows

$$\frac{q_{\text{pk}}}{\theta_{\text{pk}}} = \begin{cases} -\dfrac{K_{\text{AC}} - \theta_{\min}}{\theta_{\min} T} \ln\left(1 - \dfrac{\theta_{\min}}{K_{\text{AC}}}\right), & \theta_{\min} < K_{\text{AC}}\left(1 - e^{-1}\right), \\ \dfrac{K_{AC}e^{-1}}{\theta_{\min} T}, & \theta_{\min} \geq K_{\text{AC}}\left(1 - e^{-1}\right). \end{cases} \tag{23}$$

Through the above analysis, the parameters in equation (19) could be determined by equations (20)–(23).

4. Simulations

The following parameters are selected through analysis. $\mathbf{A}_m = \begin{bmatrix} 0 & 1 \\ -4 & -4 \end{bmatrix}$, adaptive gain $\Gamma = 10000$, low-pass filter parameter $k = 5$.

In order to examine the performance of the controller for tilt-rotor aircraft, three simulation scenarios are considered.

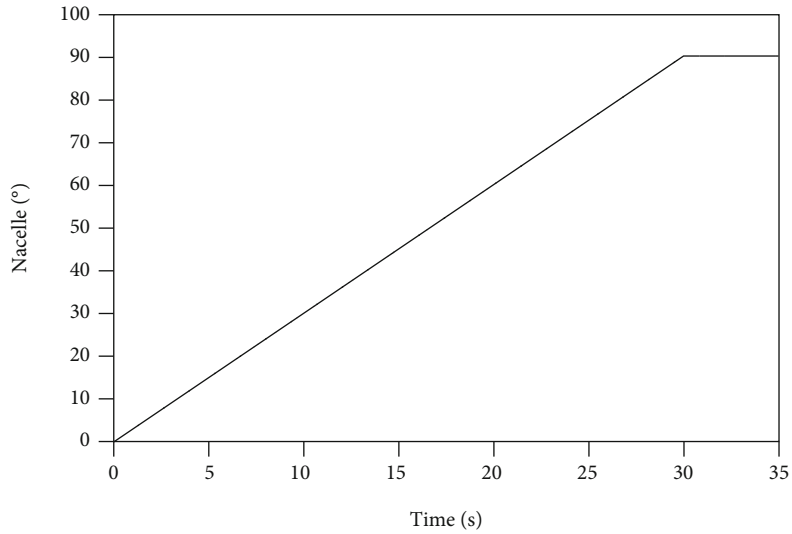

Figure 14: Nacelle angle change curve.

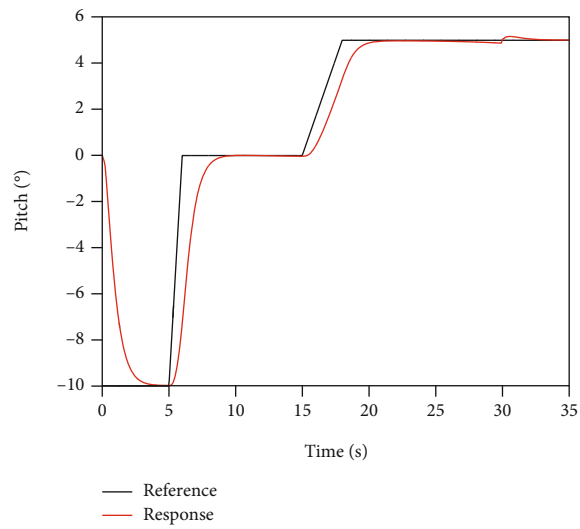

(a) Pitch angle change curve

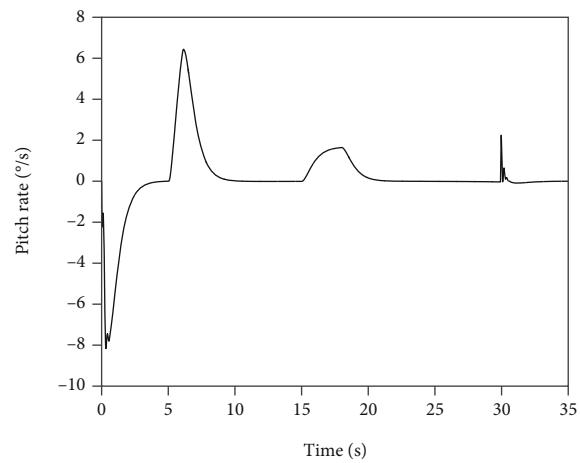

(b) Pitch rate change curve

Figure 15: The pitch angle and pitch rate change curves.

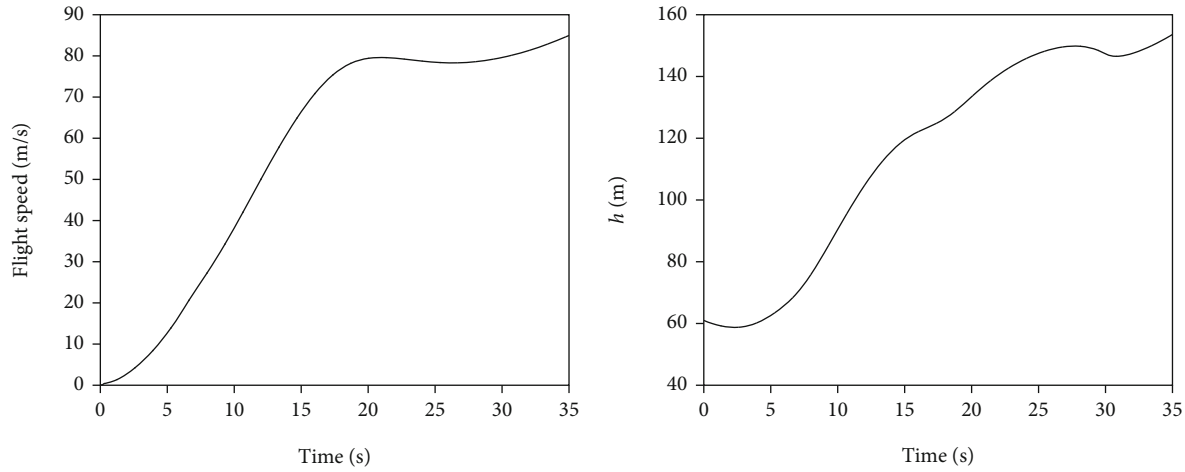

(a) Airspeed change curve (b) Height change curve

Figure 16: The airspeed and height change curves in conversion mode.

4.1. Scenario 1: Comparison with MRAC. In this case, the MRAC method was compared to verify the effectiveness of the proposed method. The simulation results for the MRAC and the proposed control methods are shown in Figures 6 and 7. It should be mentioned that the MRAC method cannot realize the attitude control of tilt-rotor aircraft in both flight modes, as shown in Figures 6(a) and 7(a). Meanwhile, the MRAC controller in experiment and simulation showed highly oscillatory behavior throughout the stimulations as observed in Figures 6(b) and 7(b), which was, of course, physically not possible.

(1) Helicopter Mode Comparison Results

(2) Airplane Mode Comparison Results

4.2. Scenario 2: Pitch Angle Capture in Certain Flight Mode. In this scenario, pitch angle capture simulations in helicopter flight mode and airplane flight mode are carrier out.

4.2.1. Pitch Angle Capture Simulation in Helicopter Mode (Hover). In this case, the head-down 10 deg task in helicopter mode is performed. The change curves of pitch rate and pitch angle are shown in Figure 8. From the figure, it can be seen that the aircraft can track the reference signal well under the action of the control system. The control signal of the aircraft is shown in Figure 9. It can be seen from the figure the low-frequency components of the control signal flow into the real system under the action of the L_1 adaptive control system. The state prediction error is shown in Figure 10. It can be found that the prediction error quickly converges under the action of the L_1 adaptive control system.

4.2.2. Pitch Angle Capture Simulation in Airplane Mode. In this case, the head-up 10 deg task in airplane mode is performed. Figure 11 shows the variations with time of the pitch rate and pitch angle for the experiment. From Figure 11(b), it can be seen that the pitch angle response can track the reference signal well. The control signal of the aircraft is shown in Figure 12. It can be seen from the figure that the frequency of the elevator signal is significantly reduced under the action of the L_1 adaptive control system. The state prediction error is shown in Figure 13, and it can be found that the prediction error quickly converges under the action of the L_1 adaptive control system.

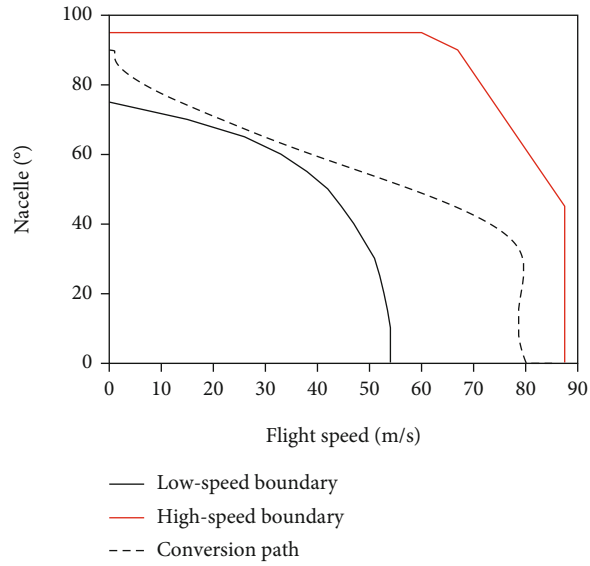

Figure 17: Conversion path curves.

4.3. Scenario 3: Automatic Conversion Simulation. Conversion mode is the most important flight mode of tilt-rotor aircraft, which has a great impact on flight safety. In order to further verify the performance of the flight control system, an automatic conversion simulation was implemented. The nacelles were assumed to rotate with a constant angular speed, as shown in Figure 14. The pitch angle command is shown in Figure 15(a) which is determined by the trim

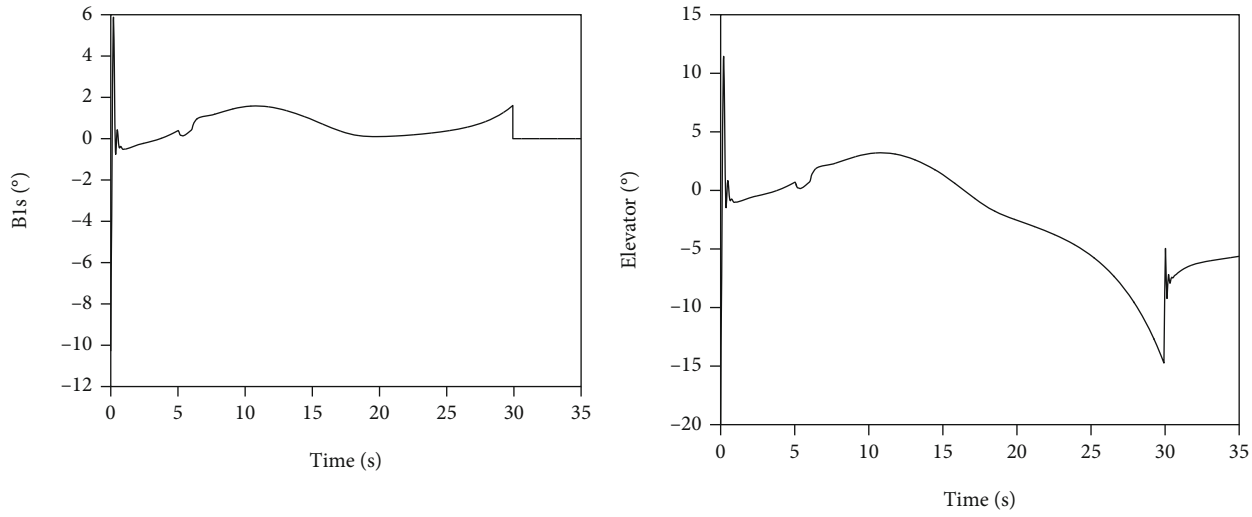

(a) Longitudinal cycle pitch change curve

(b) Elevator change curve

Figure 18: The control signal change curves.

characteristics. As we can know from Figure 15, the pitch angle response can track the reference signal well and the pitch rate changes smoothly. The change curves of its velocity and height are shown in Figure 16. It can be seen that it is an accelerated process with a certain altitude climb from helicopter mode to airplane mode. From Figure 17, the conversion path is completely in the conversion corridor, which meets the flight condition constraints of the conversion mode. The control signal of the aircraft is shown in Figure 18. It can be seen from the figure that the signals of the longitudinal cycle pitch and elevator could be physically implemented. In general, under the action of the L_1 adaptive control system, the states and control signals in the whole conversion process are reasonable.

In this section, three sets of simulation tests have been completed. It can be obtained from the first set simulation that the control method in this paper can track pitch commend in different flight modes, while MRAC cannot complete this simulation task. The second test shows that the control method in this paper can achieve good flight quality, and the control signal can be physically realized. The following conclusion can be drawn from the third set of tests is that the proposed method can realize automatic transition flight.

In addition, in the three sets of simulation tests, exactly the same controller architecture and parameter setting are selected, which avoids the repeated design of the control law and reduces the workload of the control system design.

5. Conclusions

In this paper, a L_1 adaptive controller for tilt-rotor aircraft has been proposed. The effectiveness of the controller is verified through simulation. The main conclusions are summarized as follows.

(1) Tilt-rotor aircraft has three flight modes in the flight envelope, which results in a large uncertainty in the flight dynamics model. Considering the modeling uncertainty, tilt-rotor aircraft is described as a form with unmodeled dynamics, and the L_1 adaptive control system scheme is formed

(2) The MRAC method was compared to verify the effectiveness of the proposed method. The controller in this paper can track pitch commend in different flight modes, while MRAC task failed

(3) The simulation test of the conversion flight is completed with the same controller architecture and parameters setting. The conversion from helicopter mode to airplane mode is successfully realized, which significantly reduced the workload of control law design

(4) In the future work, we will plan to implement the designed algorithm in practical application by conducting scientific experiments

Data Availability

For data availability, if the researcher needs data of this manuscript, the corresponding author can provide the data upon request.

Conflicts of Interest

The authors declare that there is no conflict of interest regarding the publication of this paper.

Acknowledgments

This work was supported by the Aeronautical Science Foundation of China (Grant Nos. 20185702003 and 201957002001).

References

[1] Anon, *Handling Qualities Requirements for Military Rotorcraft, Performance Specification, ADS-33-PRF, USAAMC*, Aviation Engineering Directorate, 2000.

[2] T. Yomchinda, J. Horn, and N. Cameron, "Integrated flight control design and handling qualities analysis for a tilt rotor aircraft," in *AIAA Atmospheric Flight Mechanics Conference*, Chicago, 2009.

[3] C. Malpica, C. R. Theodore, B. Lawrence, C. L. Blanken, and J. Lindsey, "Handling qualities of the large civil tiltrotor in hover using translational rate command," in *American Helicopter Society 68th Annual Forum*, Fort Worth, TX, 2012.

[4] T. Berger, C. L. Blanken, M. B. Tischler, and J. F. Horn, "Flight control design and simulation handling qualities assessment of high-speed rotorcraft," in *Vertical Flight Society 75th Annual Forum & Technology Display*, Philadelphia, 2019.

[5] O. Juhasz, *Flight Dynamics Simulation Modeling and Control of a Large Flexible Tiltrotor Aircraft*, Dissertation. University of Maryland, College Park, 2014.

[6] Y.-J. Lin, T.-S. Hwang, C.-C. Peng, C.-Y. Chang, and W.-R. Lai, "Neural network path tracking and real-time multitask flight simulation for the automatic transition of tiltrotor aircraft," in *Proceedings of 8th Asian Control Conference (ASCC)*, Kaohsiung, Taiwan, 2011.

[7] R. T. Rysdyk and A. J. Calise, "Adaptive model inversion flight control for tiltrotor aircraft," *Journal of Guidance, Control, and Dynamics*, vol. 22, no. 3, pp. 402–407, 1999.

[8] S. W. Choi, M. K. Lee, S. Chang, and J. M. Kim, "Development of practical tiltrotor UAV," in *50th AIAA Aerospace Sciences Meeting including the New Horizons Forum and Aerospace Exposition*, Nashville, 2012.

[9] J. H. Lee, B. M. Min, and E. T. Kim, "Autopilot design of tiltrotor UAV using particle swarm optimization method," in *International Conference on Control, Automation and Systems*, pp. 1629–1633, Korea, 2007.

[10] J. Zhang, S. U. Liguo, Q. U. Xiangju, and W. A. Liuping, "Time-varying linear control for tiltrotor aircraft," *Chinese Journal of Aeronautics*, vol. 31, no. 4, pp. 632–642, 2018.

[11] Y. Zou, C. Liu, and K. Lu, "Extended state observer based smooth switching control for tilt-rotor aircraft," *Journal of Systems Engineering and Electronics*, vol. 99, pp. 1–11, 2020.

[12] Y. Wang, C. K. Ahn, H. Yan, and S. Xie, "Fuzzy control and filtering for nonlinear singularly perturbed Markov jump systems," *IEEE Transactions on Cybernetics*, vol. 51, no. 1, pp. 297–308, 2020.

[13] Y. Wang, H. Pu, P. Shi, C. K. Ahn, and J. Luo, "Sliding mode control for singularly perturbed Markov jump descriptor systems with nonlinear perturbation," *Automatica*, vol. 127, no. 1, p. 109515, 2021.

[14] C. Cao and N. Hovakimyan, "L1 adaptive controller for nonlinear systems in the presence of unmodelled dynamics: part II," in *AmericanControl Conference*, pp. 4099–4104, Piscataway, NJ, 2008.

[15] C. Cao and N. Hovakimyan, "Design and analysis of a novel ${\cal L}_1$ adaptive control architecture with guaranteed transient performance," *IEEE Transactions on Automatic Control*, vol. 53, no. 2, pp. 586–591, 2008.

[16] N. Hovakimyan and C. Cao, *L1 Adaptive Control Theory: Guaranteed Robustness with Fast Adaptation*, SIAM, Philadelphia, PA, 2010.

[17] D. Erdos, T. Shima, E. Kharisov, and N. Hovakimyan, "L1 adaptive control integrated missile autopilot and guidance," in *AIAA guidance, navigation, and control conference*, Minneapolis, 2012.

[18] P. A. Ioannou, A. M. Annaswamy, K. S. Narendra et al., "L1-adaptive control: stability, robustness, and interpretations," *IEEE Transactions on Automatic Control*, vol. 59, no. 11, pp. 3075–3080, 2014.

[19] Z. Zuo and P. Ru, "Augmented L₁ adaptive tracking control of quad-rotor unmanned aircrafts," *IEEE Transactions on Aerospace and Electronic Systems*, vol. 50, no. 4, pp. 3090–3101, 2014.

[20] M. Bichlmeier, F. Holzapfel, E. Xargay, and N. Hovakimyan, "L1 adaptive augmentation of a helicopter baseline controller," in *AIAA Guidance, Navigation, and Control (GNC) Conference*, pp. 2013–4855, Boston, 2013.

[21] S. Banerjee, M. Creagh, R. Boyce, B. Baur, Z. Wang, and F. Holzapfel, "L1 adaptive control augmentation configuration for a hypersonic glider in the presence of uncertainties," in *AIAA Guidance, Navigation, and Control Conference*, National Harbor, 2014.

[22] S. Banerjee, T. Vanyai, Z. Wang, B. Baur, and F. Holzapfel, "L1 augmentation configuration for a lateral/directional maneuver of a hypersonic glider in the presence of uncertainties," in *19th AIAA international space Planes and hypersonic systems and technologies conference*, Atlanta, 2014.

[23] J. Dodenhöft, R. Choe, K. Ackerman, F. Holzapfel, and N. Hovakimyan, "Design and evaluation of an L1 adaptive controller for NASA's transport class model," in *AIAA Guidance, Navigation, and Control Conference*, Grapevine, 2017.

[24] K. Lu, C. Liu, C. Li, and R. Chen, "Flight dynamics modeling and dynamic stability analysis of tilt-rotor aircraft," *International Journal of Aerospace Engineering*, vol. 2019, 15 pages, 2019.

[25] S. W. Ferguson, "Development and validation of a simulation for a generic tilt-rotor aircraft," *NASA Contractor Report*, Tech. Rep. article 166537, .